AN EXPERIMENTAL STUDY OF FLOW IN A NOZZLE DESIGNED TO PROVIDE A PARALLEL JET AT SUPERSONIC SPEED

THOMAS VINCENT HENNESSEY
JOHN MORGAN DUKE, JR.

COPY FOR HEAD OF POSTGRADUATE SCHOOL

MASSACHUSETTS INSTITUTE OF TECHNOLOGY
Department of Mechanical Engineering
Cambridge 39, Mass., U.S.A.

Room 1-202

September 25, 1946

Captain Buracker
Room 5-233
Massachusetts Institute of Technology
Cambridge, Massachusetts

Thesis Work of LCDR T.V. HENNESSEY, USN
LCDR J.M. DUKE, Jr., USN

Dear Captain Buracker:

The thesis by Lt. Comdrs' T. V. Hennessey and J. M. Duke, Jr. entitled "An Experimental Study of Flow in a Nozzle Designed to Provide a Parallel Jet at Supersonic Speed" was the study of Schlieren observations of the flow in a curved passage at supersonic velocity. This passage was designed in accordance with Prandtl and Meyer theory of flow around a corner. The investigation lays the ground work for further study of supersonic flows in regions of falling pressure and rising pressure. It will have a bearing on the design of wind tunnels and of diffusion in supersonic missiles. The work was intelligently and competently carried through.

Yours very truly,

/s/ Joseph H. Keenan

JHK:emc. Joseph H. Keenan

MASSACHUSETTS INSTITUTE OF TECHNOLOGY
77 Massachusetts Avenue
Cambridge, 39, Massachusetts
September 16, 1946

Professor J.S. Newell
Secretary of the Faculty
Massachusetts Institute of Technology
Cambridge, 39, Massachusetts

Dear Professor Newell,

Herewith we submit our thesis entitled "An Experimental Study of Flow in a Nozzle Designed to Provide a Parallel Jet at Supersonic Speed" in partial fulfillment of the requirements for the Degree of Master of Science in Naval Construction and Engineering at the Massachusetts Institute of Technology.

AN EXPERIMENTAL STUDY OF FLOW

IN A NOZZLE DESIGNED TO

PRODUCE A PARALLEL JET AT SUPERSONIC SPEED
(provide)

by

THOMAS V. HENNESSEY and JOHN L. DUKE, jr.
B.S., U.S. Naval Academy 1941 B.S., U.S. Naval Academy 1941

Submitted in partial fulfillment of the

requirements for the degree of

Master of Science

at the

Massachusetts Institute of Technology

1946

ACKNOWLEDGMENT

The authors wish to acknowledge their indebtedness to Professor Ernest P. Neumann of the Department of Mechanical Engineering who gave so generously of his time in advising and guiding the work of this thesis. Mr. F. Lustwerk gave freely of his time for conference and rendered valuable assistance in the necessary laboratory technique.

Professor Neumann suggested this thesis topic.

TABLE OF CONTENTS

I SUMMARY

A. Object.

To make an experimental study of the flow in a nozzle designed to provide a parallel jet at supersonic speeds.

B. Method.

A nozzle was built based upon the theory of Prandtl and Meyer for two dimensional expansion of a gas flowing around a corner at supersonic speed. This theory assumes isentropic and irrotational flow. No allowance is made for variations in the humidity.

C. Results.

1. The observed pressure ratios followed closely the curve indicated by the theoretical values.

2. There is an effective movement of the corner downward and to the left for decreasing pressure ratios. This movement causes the nozzle contour to be theoretically incorrect since the original analysis was based on a fixed corner.

3. The normal condition of flow is shockless except for a condensation shock.

D. Conclusions.

1. The assumptions of the theory; viz, isentropic and irrotational flow are too rigid for experimental and calculated values to agree.

2. The nozzle provides a parallel stream at supersonic velocity, the velocity being dependent upon the degree of expansion desired.

3. The presence of the condensation shock caused an additional variation in the observed and calculated values of pressure ratios.

E. Recommendations.

1. That the humidity be controlled.

2. That further investigation of boundary layer conditions be made when apparatus becomes available.

3. That Schlieren photographs of pressure shocks be made using a faster method of exposure.

4. That further investigation be made as to the possibility of using this nozzle contour as a supersonic diffuser.

II INTRODUCTION

The purpose of this thesis was to make an experimental study of the flow in a nozzle designed to provide a parallel jet at supersonic speed. This study was to include views of the flow with the Schlieren apparatus to determine if normal flow was shockless; to investigate the boundary layer conditions; and to determine the effect of pressure shocks occuring in the nozzle contour. So far as is known, no studies of this nature have been previously made.

Two arbitrary streamlines, as defined by the Prandtl and Meyer theory for flow around a corner were selected for the nozzle contour, the choice of streamlines being governed primarily by a limitation of the physical length of the nozzle, and the capacity of the air ejector. At the nozzle throat which is the beginning of the flow around the corner, and also the beginning of the streamline contours, the critical pressure ratio exists and sonic velocity occurs. At sections downstream from the throat expansion occurs, the pressure ratio becomes less than critical, the stream changes direction as defined by the streamlines, and the velocity becomes supersonic. Conditions at the entrance to the nozzle are atmospheric,

and the entrance area is made large enough to reduce the approach velocity to 3% of that at the throat. No attempt was made to control humidity of the air entering the nozzle.

III EXPERIMENTAL TECHNIQUE

A. Description of Nozzle.

The nozzle was machined in two separate pieces as shown in Fig. 1, the pieces being held in proper position relative to each other by straps at either end fitted with dowel pins. Pressure taps were provided at the throat section and at points of theoretical pressure ratios of 0.50, 0.40, 0.30, 0.20, 0.15 and 0.10 for both the upper and lower contours. These taps led to a battery of mercury manometers, permitting measurement of the pressure at the tap. Plate glass sides, of the general outline of the nozzle, were fitted to its sides and made air tight by a thin layer of Duco cement between glass and nozzle sides, and by tape along the edges of the glass. The exit end of the nozzle was fitted with a wooden adapter to permit connecting it to the air ejector piping.

B. Operation.

Flow of air through the nozzle is started by bringing the air ejector up to its operating point and opening the cut-out valve to the nozzle. This valve is opened wide so that shockless flow is obtained. Steady state conditions are reached quite rapidly after which readings of the manometer battery are taken. Atmospheric conditions are also recorded.

As the exhaust valve is closed, a shock will occur in the nozzle contour and further closing of this valve moves the shock toward the throat until

finally it occurs at the entrance. The position of this shock can be determined approximately from the indications of the manometer readings.

TEST APPARATUS
(Schematic)

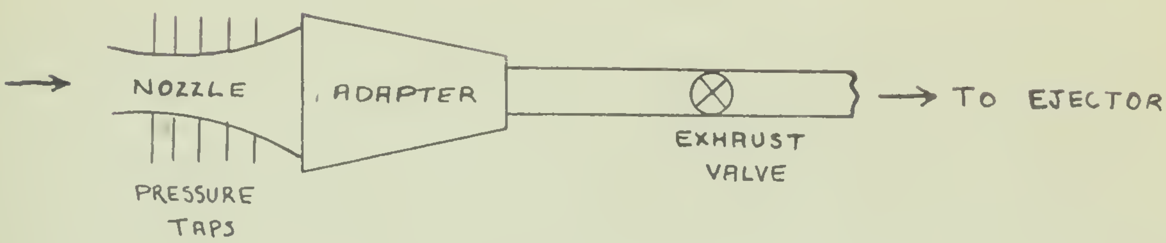

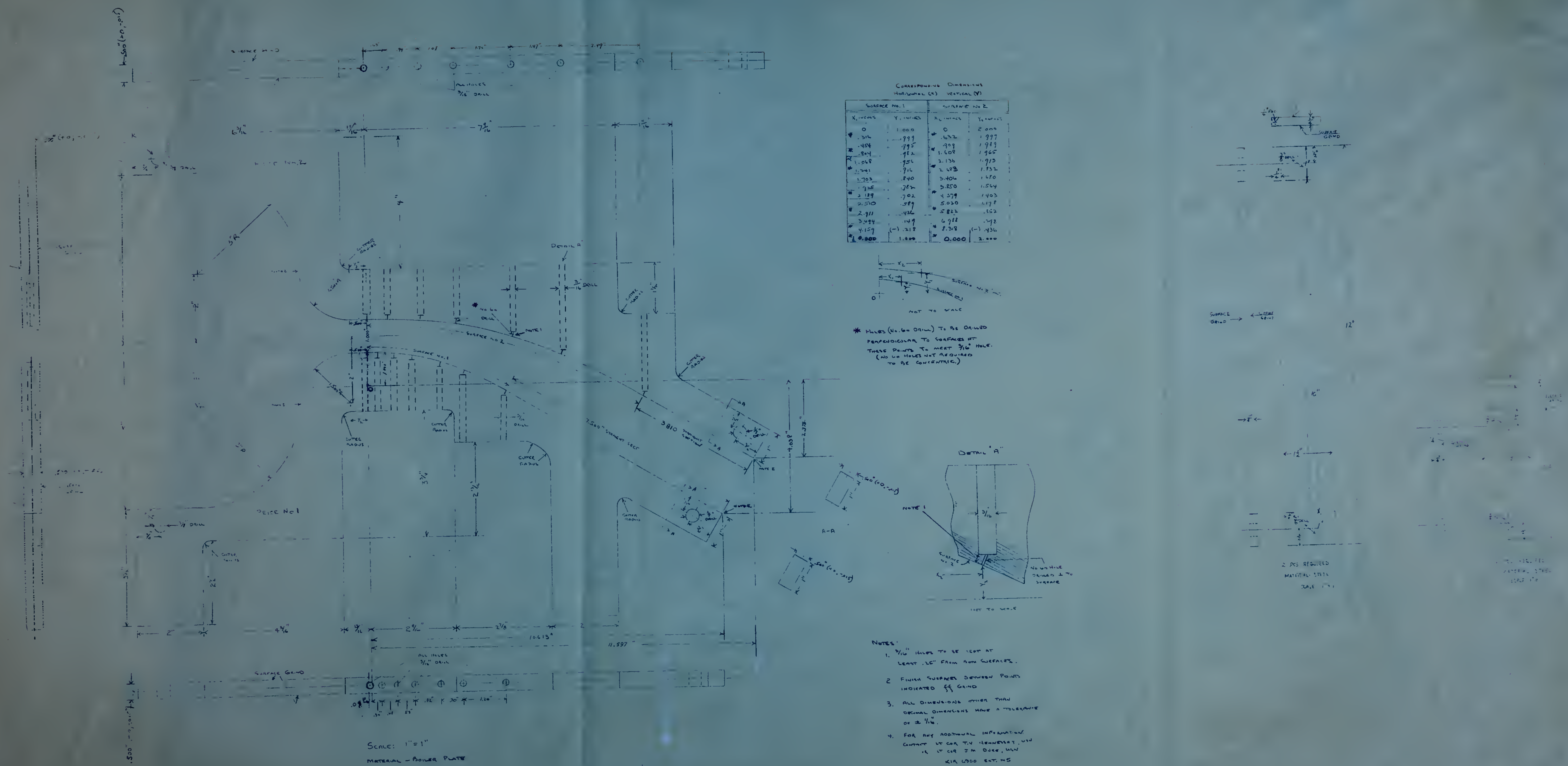

Corresponding Dimensions
Horizontal (X) Vertical (Y)

Surface No. 1		Surface No. 2	
X_1 inches	Y_1 inches	X_2 inches	Y_2 inches
0	1.000	0	2.000
* .316	.999	* .632	1.997
.454	.995	.909	1.989
* .804	.982	* 1.608	1.965
* 1.068	.956	2.136	1.913
* 1.341	.916	* 2.683	1.832
1.703	.840	3.406	1.680
1.925	.782	3.850	1.564
* 2.189	.702	* 4.379	1.403
2.510	.589	5.020	1.178
* 2.911	.426	* 5.822	.852
3.494	.149	6.988	.292
* 4.159	(−) .218	* 8.318	(−) .436
* 0.000	1.000	* 0.000	2.000

FIG. 1

IV RESULTS

Results are submitted in the form of curves shown by Figs. 2, 3, 4, 5(a), and 5(b).

A. Fig. 2 is a dimensionless plot of pressure ratio versus area ratio. It shows how nearly the actual conditions in the nozzle approach the theoretical. The curves for the bottom and top contours were based on the average values of ten separate, normal runs taken on different days. Since each plotted point is an average value, the curves were passed through all points rather than faired in.

B. Fig. 3 shows the lines of theoretical constant pressure as determined from the average readings for the ten normal runs. In general, the actual constant pressure lines do not pass through the point "O" as required by theory, and they show a movement of this point downward and to the left.

C. Fig. 4 shows the computed thickness of the boundary layer on both contours assuming that it is of equal thickness on all bounding surfaces. These curves are qualitative only.

D. Figs. 5(a) and 5(b) show the effect on the pressure ratios of shocks in the nozzle produced by increasing the exhaust pressure. Curve I represents a selected normal run; curve II represents a run with a shock in the nozzle contour; successive curves are with the shock nearer the throat. Curve VII is with the shock outside the nozzle throat.

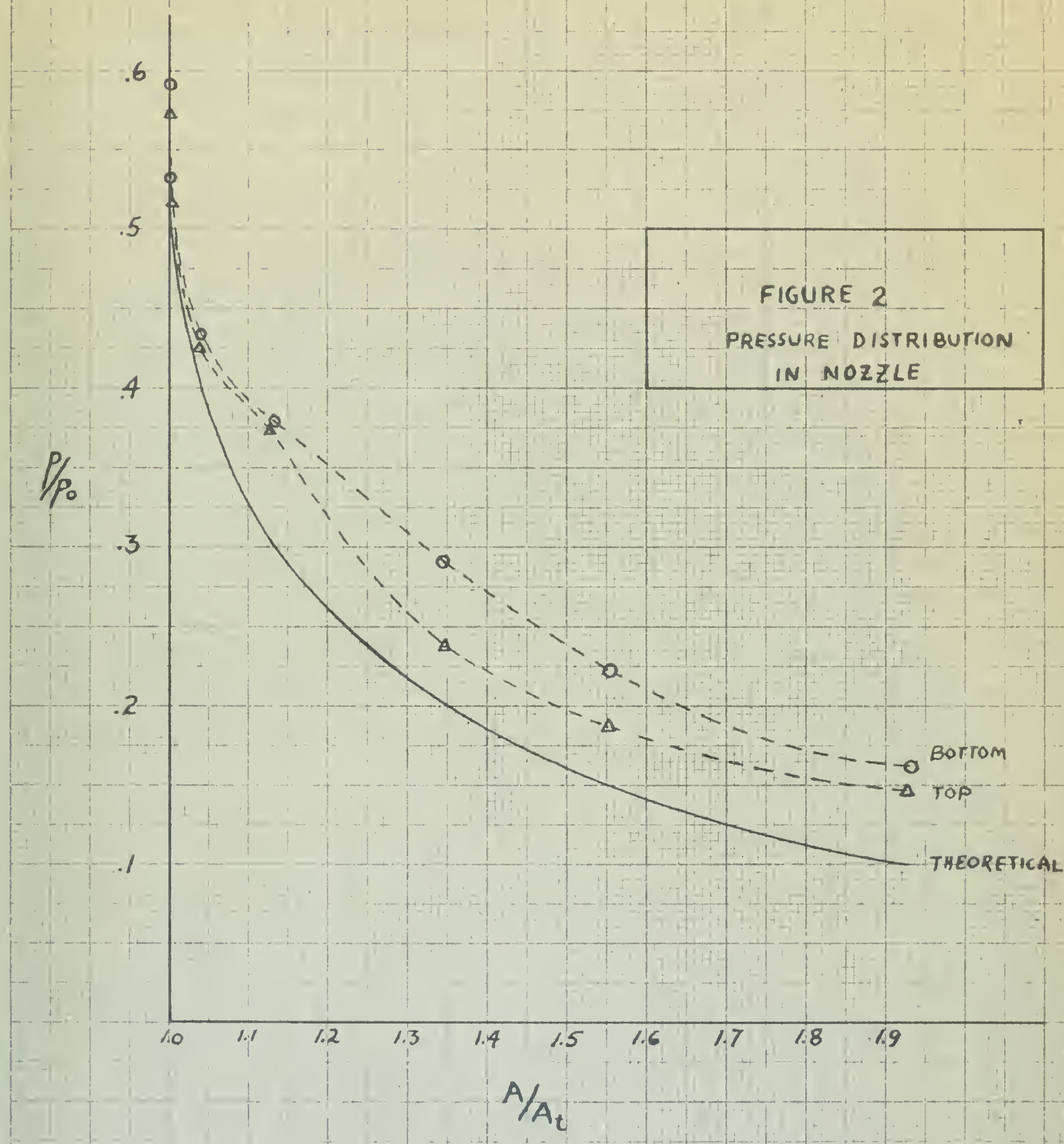
FIGURE 2
PRESSURE DISTRIBUTION
IN NOZZLE
BOTTOM
TOP
THEORETICAL
P/Po
A/At
.1
.2
.3
.4
.5
.6
1.0
1.1
1.2
1.3
1.4
1.5
1.6
1.7
1.8
1.9

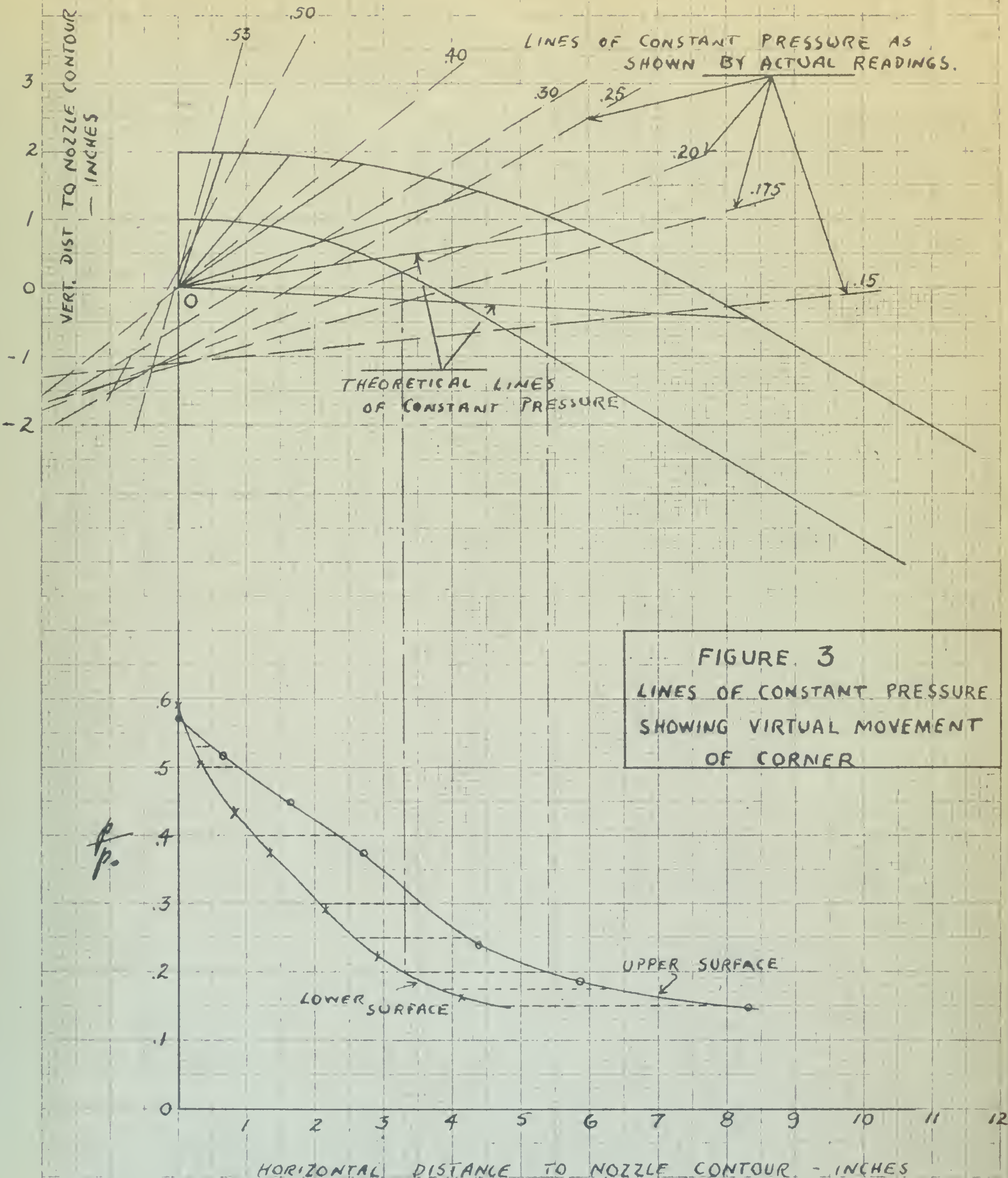

FIGURE 3
LINES OF CONSTANT PRESSURE SHOWING VIRTUAL MOVEMENT OF CORNER

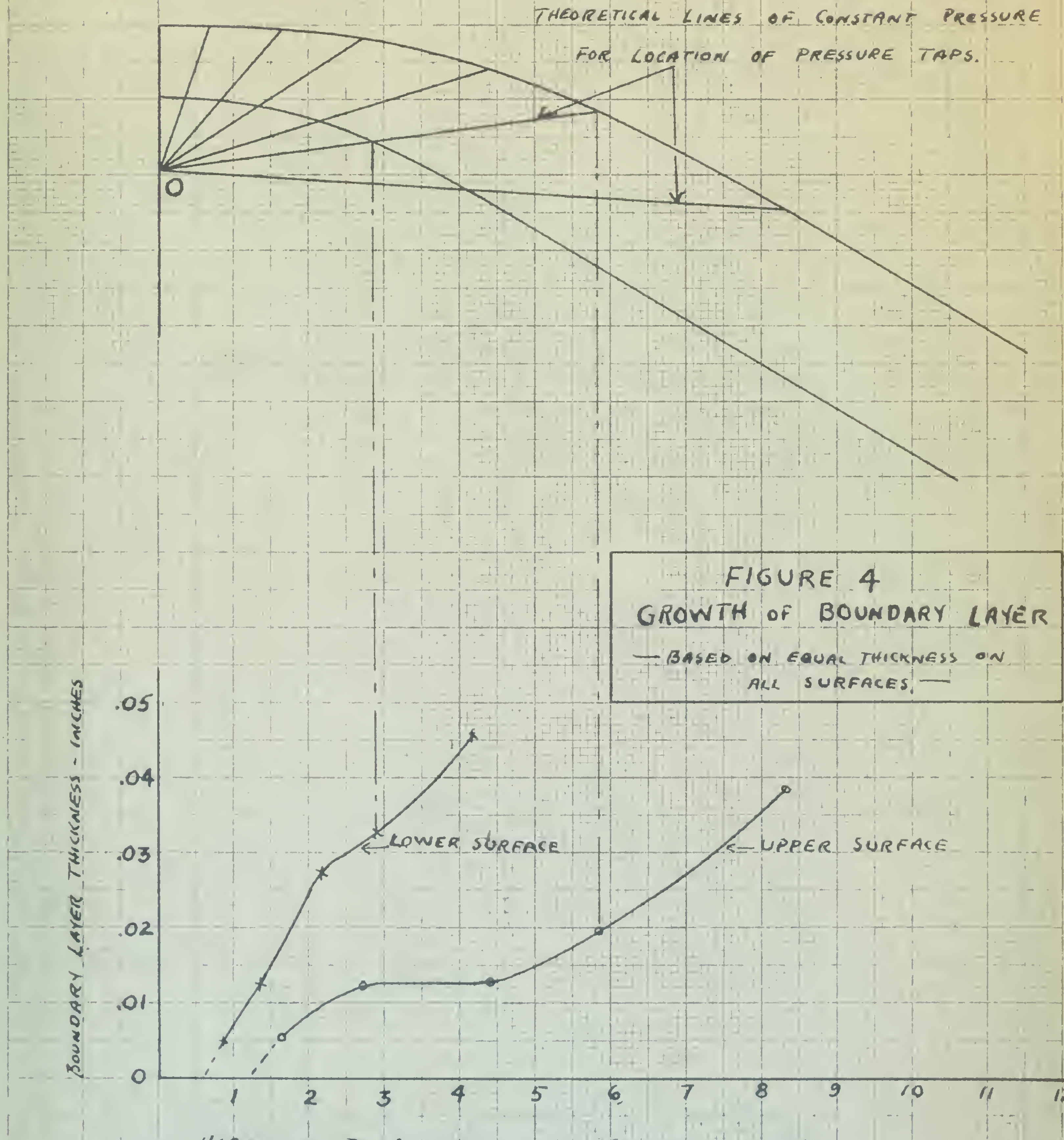
THEORETICAL LINES OF CONSTANT PRESSURE
FOR LOCATION OF PRESSURE TAPS.
O
FIGURE 4
GROWTH of BOUNDARY LAYER
— BASED ON EQUAL THICKNESS ON
ALL SURFACES. —
LOWER SURFACE
UPPER SURFACE
BOUNDARY LAYER THICKNESS - INCHES
.05
.04
.03
.02
.01
0
1
2
3
4
5
6
7
8
9
10
11
12
HORIZONTAL DISTANCE TO NOZZLE CONTOUR - INCHES

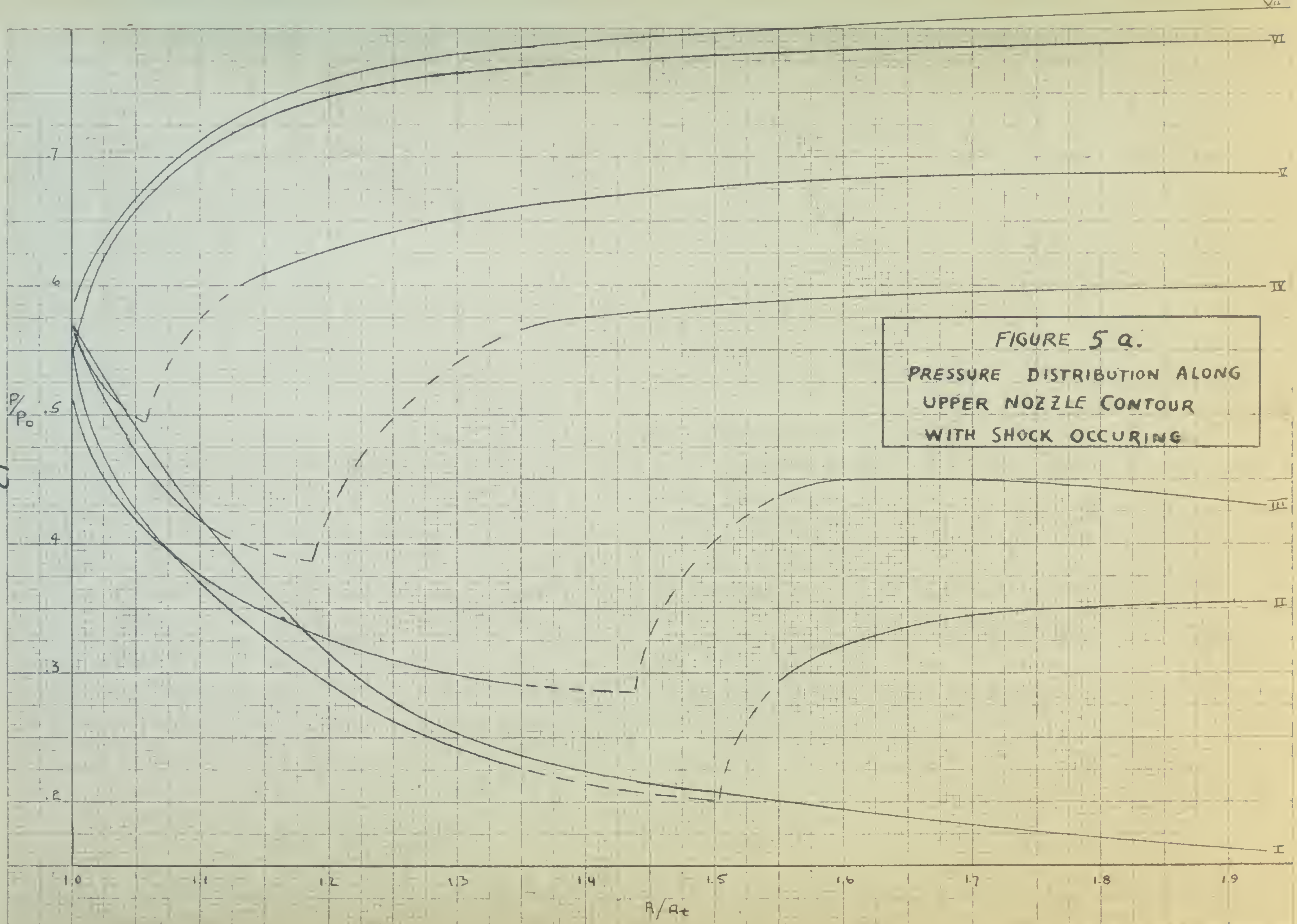

FIGURE 5 a.
PRESSURE DISTRIBUTION ALONG UPPER NOZZLE CONTOUR WITH SHOCK OCCURING

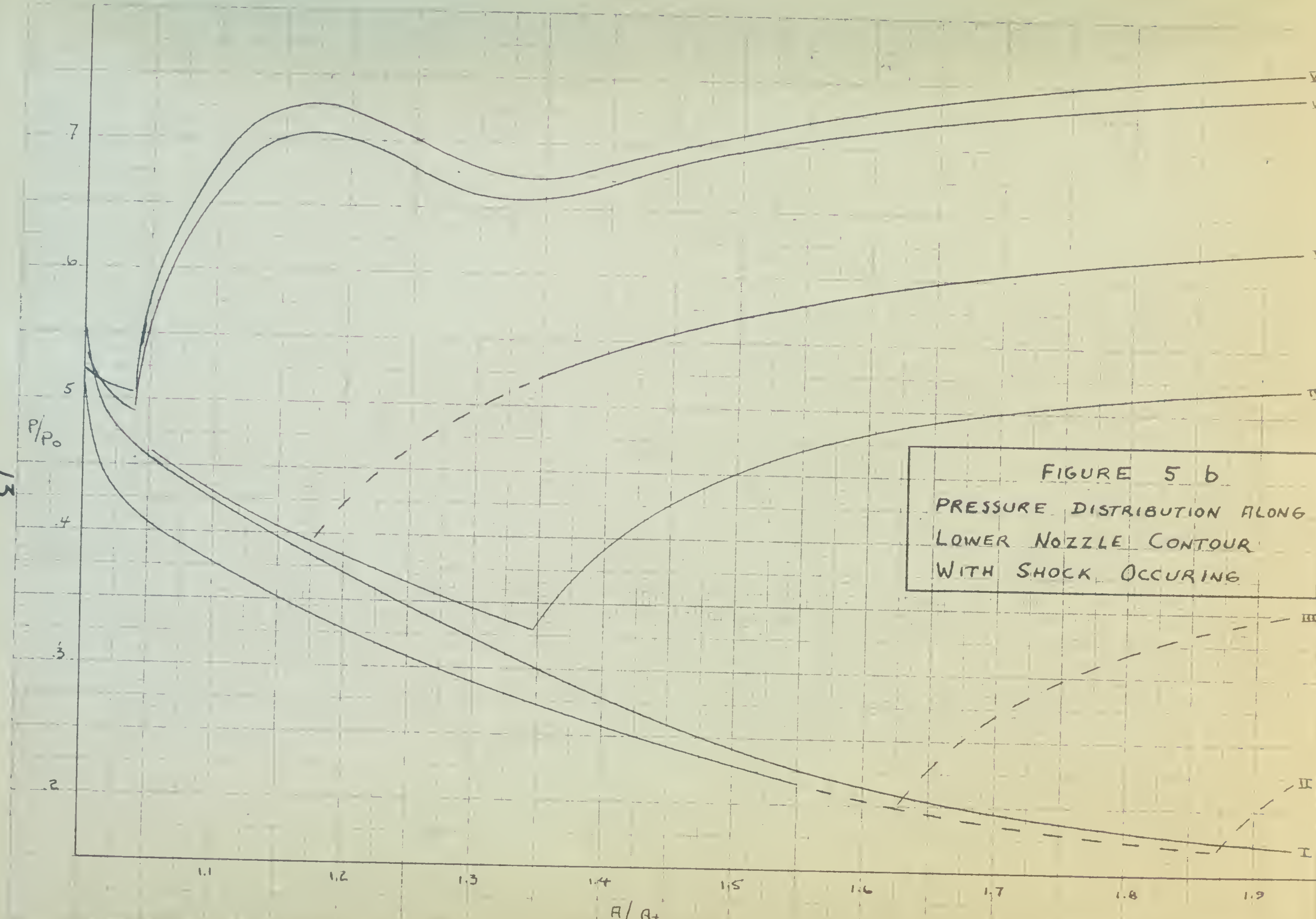

FIGURE 5 b
PRESSURE DISTRIBUTION ALONG LOWER NOZZLE CONTOUR WITH SHOCK OCCURING

V DISCUSSION OF RESULTS

A. The plot of pressure ratio existing in the nozzle versus area ratio shows that the experimental value does not reach the theoretical value. This result is as expected since the theoretical value ignores the effects of friction and the subsequent building-up of the boundary layer. In addition, the theoretical value assumes dry air and so does not have to account for the effects of condensation. In this nozzle there was a condensation shock present at all times that normal runs were made. This shock occurred in the vicinity of the 0.40 pressure ratio tap. The position of the shock varied slightly from day to day depending upon the relative humidity. A shock of this kind moves downstream from the throat as relative humidity decreases, and as the relative humidity approaches zero, the flow in a nozzle approaches isentropic conditions more closely (4).

The effect of the condensation shock on pressure ratio is shown by the rise of the curves in the region between the taps for pressure ratios of 0.40 and 0.20. This effect is more noticeable along the upper contour than it is along the lower contour.

At the beginning of the straight section the pressure ratios are becoming more nearly the same for upper and lower contours.

B. For the construction of Fig. 3 a plot of the nozzle contour was made, and the lines of theoretical constant pressure, where pressure taps were located, were drawn in. Then the average pressure ratio readings for normal runs were plotted vertically below their corresponding taps. From these points the curves of pressure ratio versus horizontal distance along the nozzle contour were drawn for both the upper and lower surfaces. Since a line of constant pressure is a horizontal line on this plot, by projecting vertically upward, the points of equal pressure may be located on both the nozzle surfaces. However, the Schlieren pictures show that the pressure is not constant along the line connecting points of equal pressure, nor along any radial line in the nozzle contour, but rather that a line of constant pressure, as indicated by the shock, is a line concave downstream. The average slope of the shock is such that the tangent will pass near "O".

These lines, connecting points of equal pressure, depart from the theoretical lines of constant pressure and, in general, show a rotation about the original lines. The result is an effective movement of the corner showing that the nozzle contour is no longer correct even if isentropic flow were realized.

From this plot, the location of the throat is shown to be very near the tap for a pressure ratio of 0.50. Actually, the throat section of the nozzle was

not in the proper location. While assembling the nozzle it was discovered that the section of minimum area was between the 0.53 and 0.50 pressure ratio taps, being closer to the 0.50 tap. An attempt was made to correct this condition by rubbing the surface with emery and crocus cloth, but the result was not completely successful. The difference in area between the pressure taps at 0.53 and those at 0.50 is very critical being of the order of 0.0009 in^2. Thus very slight errors in machining the nozzle contours will result in variation in the position of the throat.

Calculations were made for the vertical movement of "O" using the theoretical relations developed in Appendix B, the observed values of pressure ratio, and the geometry of the figure. These calculations show the same movement of "O" as is shown in the plot, so they are not included here. They may be found in the original data.

Using the theoretical relations and plotting a new contour based on the new position of "O" showed that the nozzle as actually made had too much curvature. In operation this was indicated by the formation of a film of grease and dust on the upper surface.

C. Originally, it was intended to study the boundary layer with Schlieren apparatus designed for this work in an effort to obtain quantitative results.

However, this apparatus was not completed in time to enable the study to be made.

Qualitative results were obtained by assuming that the thickness of the boundary layer on the glass sides and the nozzle contour is the same. The difference between the area required to expand isentropically to the observed pressure ratio and the area existing in the nozzle at this ratio was taken as the area of the boundary layer. As the pressures at corresponding taps on upper and lower surfaces were not identical, boundary layer thicknesses were computed using data from each contour. The two curves obtained indicate that the boundary layer thickness is not the same for upper and lower contours, which invalidates the original assumption, but they do show an increase in thickness with distance along the contour.

An attempt was made to compute thicknesses based on the movement of the corner, but no significant results were obtained. These calculations are with the original data.

D. The location of the shocks introduced in the nozzle contour was not determined exactly. From a consideration of the manometer readings and the Schlieren pictures, an approximate location can be deduced. The curves are shown dotted where shocks occured since these points are doubtful.

The curves for the top contour are conventional

in that when a shock occurs there is an abrupt pressure rise across the shock with the pressure continuing to rise after the shock.

Curves for the bottom contour are conventional except for runs VI and VII for which there is an abrupt pressure rise followed by a decrease in pressure and then an increase in pressure. It is not known what causes this peculiar behavior of the lower contour for shocks at or near the entrance. However, the shock in both these runs occurred in the vicinity of the condensation shock which may have affected the readings in some manner. If this were the case, it seems reasonable to expect that the pressure taps along the upper contour would show the same effect. Since the upper contour does not show the same result, possibly the fact that the pressure taps are a greater distance apart along that surface allows the flow to become stable before reaching the next tap.

VI CONCLUSIONS

1. The flow is not isentropic.
2. Pressure is not constant along a radial line.
3. The condensation shock was not anticipated and may have had considerable effect on the results.
4. A new, theoretical contour based on the movement of "O" showed that the original contour had too much curvature.

VII RECOMMENDATIONS

1. That the humidity be controlled.

2. That further investigation of boundary layer conditions be made when apparatus becomes available with a view to obtaining quantitative results.

3. That Schlieren photographs of shocks be made using faster methods of exposure.

4. That further investigation be made as to the possibility of using this nozzle contour as a supersonic diffuser.

5. That the throat be located directly above "O".

APPENDIX

VIII APPENDIX

A. Symbols

A Area perpendicular to flow at any point.

A_t Throat area.

a Local velocity of sound.

c Velocity which a gas would attain if allowed to flow in steady motion into a vacuum.

G Mass rate of flow.

k Ratio of specific heats (1.400).

M Mach number.

m Local Mach angle.

O Origin for rectangular and polar coordinates; corner about which expansion is assumed to take place.

O' Corner about which expansion actually takes place.

p Absolute pressure at point considered.

p_{cr} Critical pressure ratio.

p_o Atmospheric pressure.

p_o' Stagnation pressure at section O.

q Stream velocity at any point.

r Radius vector to any point from "O".

r' Radius vector to any point from O'.

r_1 Radius vector at throat.

r_1' Radius vector at throat from O'.

r_2 Radius vector at point 2 from O.

Δr_1 Radial distance at throat between selected streamlines.

Δr_2 Radial distance at point 2 between selected streamlines.

T Absolute temperature at any point.

u Component of stream velocity along radius vector at any point.

v Component of stream velocity perpendicular to radius vector at any point.

v_{sub} Specific volume at any point considered.

x Abscissa at any point considered.

y Ordinate at any point considered.

z Vertical movement of O.

λ A constant $= \sqrt{\frac{k-1}{k+1}}$

θ Angle at O between vertical and radius vector to any point.

θ' Angle at O' between vertical and radius vector to any point.

ψ Complement of local mach angle.

ρ Stream density.

B. Development of Theoretical Equations

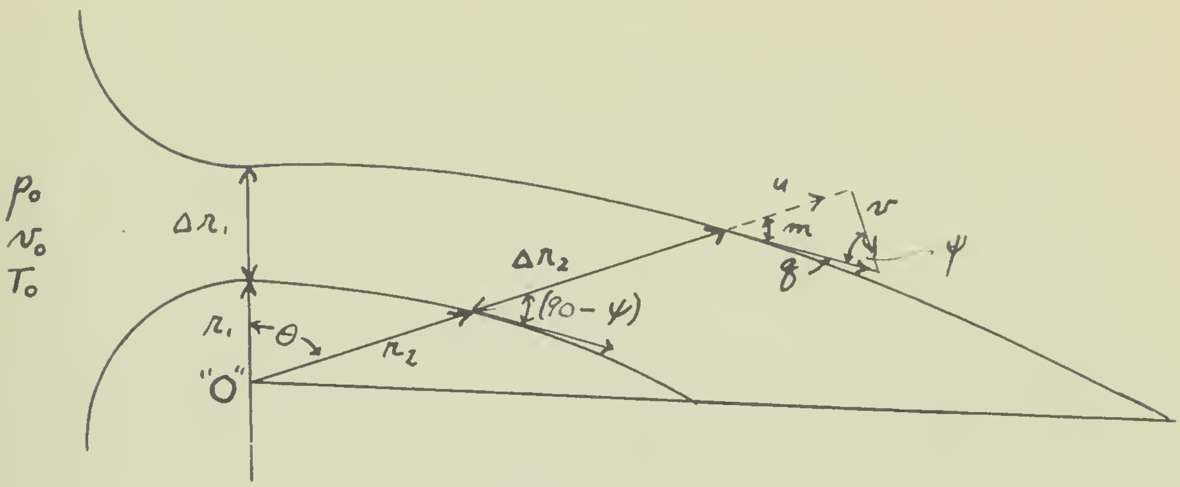

The dynamic equations for any two dimensional fluid motion expressed in polar coordinates are

$$u\frac{\partial u}{\partial r} + \frac{v}{r}\frac{\partial u}{\partial \theta} - \frac{v^2}{r} = -\frac{1}{\rho}\frac{\partial p}{\partial r} \tag{1}$$

$$u\frac{\partial v}{\partial r} + \frac{v}{r}\frac{\partial v}{\partial \theta} + \frac{uv}{r} = -\frac{1}{\rho}\frac{\partial p}{r\,\partial \theta} \tag{2}$$

where u and v are the components of velocity along and perpendicular to the radius vector through the point considered.

The equation of continuity is

$$\frac{\partial}{\partial r}(\rho u r) + \frac{\partial}{\partial \theta}(\rho v) = 0 \tag{3}$$

Assume: 1. Velocity, pressure and density are constant along a radius.

2. Isentropic conditions.

Then (1), (2) and (3) reduce to

$$v = \frac{du}{d\theta} \tag{4}$$

$$\frac{v}{r}\left(\frac{dv}{d\theta} + u\right) = -\frac{1}{\rho}\frac{dp}{r\,d\theta} \tag{5}$$

$$\rho u + \frac{d}{d\theta}(\rho v) = 0 \tag{6}$$

Equation (4) is the condition for irrotational flow and shows that this type of motion is implied.

Since $\dfrac{d\rho}{d\theta} = \dfrac{1}{a^2}\dfrac{dp}{d\theta}$, (5) may be written as

$$\frac{v}{r}\left(\frac{dv}{d\theta} + u\right) = -\frac{a^2}{\rho}\frac{d\rho}{r\,d\theta} \tag{7}$$

Substituting in (6) the value of $\dfrac{d\rho}{d\theta}$

$$\left(\frac{dv}{d\theta} + u\right)\left(1 - \frac{v^2}{a^2}\right) = 0 \tag{8}$$

which is the general equation of flow which must be satisfied. Since $\left(\dfrac{dv}{d\theta} + u\right)$ cannot be 0 for all values of θ, as the pressure would then be constant throughout the field, we must have

$$a^2 = v^2 \quad \text{or} \quad a = v \tag{9}$$

and from the adiabatic law

$$a^2 = \frac{kp}{\rho} = v^2 \tag{10}$$

From Bernoulli's equation we have

$$\frac{1}{2}(u^2 + v^2) + \frac{k}{k-1}\frac{p}{\rho} = \frac{k}{k-1}\frac{p_0}{\rho_0} = \frac{1}{2}c^2 \tag{11}$$

substituting the value of v^2 from (10) in (11)

$$u^2 + \frac{k+1}{k-1} v^2 = c^2 \tag{12}$$

substituting the value of v from (4) in (12)

gives
$$\left(\frac{du}{d\theta}\right)^2 = \lambda^2 (c^2 - u^2) \tag{13}$$

where
$$\lambda^2 = \frac{k-1}{k+1}$$

Integration of (13) with θ measured from the radius at which u=0 so that the constant of integration will vanish gives

$$\lambda\theta = \sin^{-1}\left(\frac{u}{c}\right)$$

or
$$u = c \sin \lambda\theta \tag{14}$$

$$v = \frac{du}{d\theta} = c\lambda \cos \lambda\theta \tag{15}$$

From equations (10) and (11) we have

$$q^2 = u^2 + v^2 = \frac{2k}{k-1} \frac{p_0}{\rho_0} \left[1 - \left(\frac{p}{p_0}\right)^{\frac{k-1}{k}}\right] \tag{16}$$

From condition that mass rate of flow is a constant

$$G = \frac{q_1 \Delta r_1}{v_1} = \frac{q_2 \Delta r_2 \sin(90 - \psi)}{v_2} \tag{17}$$

and remembering $\frac{\Delta r_1}{r_1} = \frac{\Delta r_2}{r_2}$, we obtain

$$r_2 = \frac{v_2}{v_1} \frac{q_1}{q_2} \frac{r_1}{\cos\psi} \tag{18}$$

From the adiabatic gas law

$$\frac{v_2}{v_1} = \frac{\left(\frac{p_1}{p_0}\right)^{\frac{1}{k}}}{\left(\frac{p_2}{p_0}\right)^{\frac{1}{k}}} \tag{19}$$

from equation (16)

$$\frac{q_1}{q_2} = \frac{\left[1-\left(\frac{p_1}{p_0}\right)^{\frac{k-1}{k}}\right]^{\frac{1}{2}}}{\left[1-\left(\frac{p_2}{p_0}\right)^{\frac{k-1}{k}}\right]^{\frac{1}{2}}}$$

then (18) becomes

$$r_2 = \frac{\left(\frac{p_1}{p_0}\right)^{\frac{1}{k}}\left[1-\left(\frac{p_1}{p_0}\right)^{\frac{k-1}{k}}\right]^{\frac{1}{2}} r_1}{\left(\frac{p_2}{p_0}\right)^{\frac{1}{k}}\left[1-\left(\frac{p_2}{p_0}\right)^{\frac{k-1}{k}}\right]^{\frac{1}{2}} \cos\psi} \qquad (20)$$

From the figure

$$\tan\psi = u/v$$

$$\tan\psi = \frac{\sin\lambda\theta}{\lambda\cos\lambda\theta}$$

$$\tan\psi = \frac{1}{\lambda}\tan\lambda\theta \qquad (21)$$

$$1+\tan^2\psi = \sec^2\psi$$

$$1+\frac{1}{\lambda^2}\tan^2\lambda\theta = \sec^2\psi$$

$$\cos^2\psi = \frac{\lambda^2}{\lambda^2+\tan^2\lambda\theta}$$

$$\cos\psi = \left[\frac{\lambda^2}{\lambda^2+\tan^2\lambda\theta}\right]^{\frac{1}{2}} \qquad (22)$$

From equations (14), (15) and (16)

$$q^2 = u^2+v^2 = \frac{2k}{k-1}\frac{p_0}{\rho_0}\left[1-\left(\frac{p}{p_0}\right)^{\frac{k-1}{k}}\right]$$

$$q^2 = c^2\left[\sin^2\lambda\theta + \lambda^2\cos^2\lambda\theta\right]$$

$$q^2 = c^2\left[1-\frac{1}{2}(1-\lambda^2)(1+\cos 2\lambda\theta)\right] \qquad (23)$$

by substituting (23) in (16) and remembering

that $c^2 = \frac{2k}{k-1}\frac{p_0}{\rho_0}$ and $\frac{1}{2}(1-\lambda^2) = \frac{1}{k+1}$

we obtain $\left(\frac{p}{p_0}\right)^{\frac{k-1}{k}} = \frac{1}{k+1}(1+\cos 2\lambda\theta)$ (24)

$$\cos 2\lambda\theta = (k+1)\left(\frac{p}{p_o}\right)^{\frac{k-1}{k}} - 1$$

$$\cos 2\lambda\theta = 2\cos^2\lambda\theta - 1$$

$$\left[2\cos^2\lambda\theta - 1\right] = \left[(k+1)\left(\frac{p}{p_o}\right)^{\frac{k-1}{k}} - 1\right]$$

$$\cos^2\lambda\theta = \frac{k+1}{2}\left(\frac{p}{p_o}\right)^{\frac{k-1}{k}} \qquad (25)$$

$$\sec^2\lambda\theta = \tan^2\lambda\theta - 1$$

$$\tan^2\lambda\theta = \left[\left(\frac{2}{k+1}\right)\left(\frac{p_o}{p}\right)^{\frac{k-1}{k}} - 1\right] \qquad (26)$$

substituting (26) in (22) and squaring

$$\cos^2\psi = \frac{\lambda^2}{\left[\lambda^2 + \frac{2}{k+1}\left(\frac{p_o}{p}\right)^{\frac{k-1}{k}} - 1\right]} \qquad (27)$$

substituting value of λ in (27) and solving for $\cos\psi$ at any point in terms of the pressure gives

$$\cos\psi = \left(\frac{k-1}{2}\right)^{\frac{1}{2}}\left[\left(\frac{p_o}{p}\right)^{\frac{k-1}{k}} - 1\right]^{\frac{1}{2}} \qquad (28)$$

substituting the value of $\cos\psi$ at r_2 from (28) in (20)

$$r_2 = r_1\left(\frac{p_1}{p_o}\right)^{\frac{1}{k}}\left(\frac{p_2}{p_o}\right)^{\frac{1}{k}}\frac{\left[1-\left(\frac{p_1}{p_o}\right)^{\frac{k-1}{k}}\right]^{\frac{1}{2}}\left[\left(\frac{p_o}{p_2}\right)^{\frac{k-1}{k}} - 1\right]^{\frac{1}{2}}}{\left[1-\left(\frac{p_2}{p_o}\right)^{\frac{k-1}{k}}\right]^{\frac{1}{2}}\left(\frac{k-1}{2}\right)^{\frac{1}{2}}} \qquad (29)$$

taking two of terms from above equation and simplifying

$$\frac{\left[\left(\frac{p_o}{p_2}\right)^{\frac{k-1}{k}} - 1\right]^{\frac{1}{2}}}{\left[1-\left(\frac{p_2}{p_o}\right)^{\frac{k-1}{k}}\right]^{\frac{1}{2}}} = \left(\frac{p_2}{p_o}\right)^{-\frac{k-1}{2k}}$$

Since velocity is sonic at section 1 (throat)

$$\frac{p_1}{p_0'} = p_{cr} = \left(\frac{2}{k+1}\right)^{\frac{k}{k-1}}$$

(velocity at $p_0 \approx 0$ so $p_0 = p_0'$)

(where p_0' = stagnation pressure at section 0)

taking terms in $\left(\frac{p_1}{p_0}\right)$ from (29)

$$\left(\frac{p_1}{p_0}\right)^{\frac{1}{k}}\left[1-\left(\frac{p_1}{p_0}\right)^{\frac{k-1}{k}}\right]^{\frac{1}{2}} = \left(\frac{2}{k+1}\right)^{\frac{1}{k-1}}\left(\frac{k-1}{k+1}\right)^{\frac{1}{2}}$$

since r_2 is any radius, drop the subscript and let $r_2 = r$. (29) then becomes

$$r = r_1\left(\frac{2}{k+1}\right)^{\frac{1}{k-1}}\left(\frac{k-1}{k+1}\right)^{\frac{1}{2}}\left(\frac{2}{k-1}\right)^{\frac{1}{2}}\left(\frac{p}{p_0}\right)^{-\frac{k+1}{2k}} \qquad (30)$$

from (24) $\frac{p}{p_0} = \left[\frac{2}{k+1}\left(\cos^2 \lambda\theta\right)\right]^{\frac{k}{k-1}}$

$$\left(\frac{p}{p_0}\right)^{-\frac{k+1}{2k}} = \left[\frac{2}{k+1}\left(\cos^2\lambda\theta\right)\right]^{-\frac{k+1}{2(k-1)}} \qquad (31)$$

substituting (31) in (30) and sumplifying

$$r = r_1\left(\cos\lambda\theta\right)^{-\frac{k+1}{k-1}} \qquad (32)$$

or directly from (30)

$$r = r_1\left(\frac{2}{k+1}\right)^{\frac{k+1}{2(k-1)}}\left(\frac{p}{p_0}\right)^{-\frac{k+1}{2k}} \qquad (33)$$

from (25)

$$\cos\lambda\theta = \left[\frac{k+1}{2}\left(\frac{p}{p_0}\right)^{\frac{k-1}{k}}\right]^{\frac{1}{2}}$$

$$\theta = \frac{1}{\lambda}\left\{\cos^{-1}\left[\frac{k+1}{2}\left(\frac{p}{p_0}\right)^{\frac{k-1}{k}}\right]^{\frac{1}{2}}\right\}$$

$$\theta = \left(\frac{k+1}{k-1}\right)^{\frac{1}{2}}\cos^{-1}\left[\frac{k+1}{2}\left(\frac{p}{p_0}\right)^{\frac{k-1}{k}}\right]^{\frac{1}{2}} \qquad (34)$$

Using value of k as 1.4000, (33) and (34) reduce to

$$r = 0.57871\, r_1 \left(\frac{p}{p_0}\right)^{-0.85714} \tag{35}$$

$$\theta = 2.44949 \cos^{-1}\left[1.0954\left(\frac{p}{p_0}\right)^{0.14286}\right] \tag{36}$$

By substituting values of $\left(p/p_0\right)$ in equations (21), (35) and (36), the following values of r, θ and ψ were obtained for plotting the streamlines. (See TABLE I on following page.)

For ease of laying out the contour, the dimensions as given in TABLE I were changed from polar to rectangular coordinates as shown on the sketch of the nozzle (Figure 1). The origin for the rectangular coordinates is the corner about which the expansion is assumed to take place.

The straight section of the nozzle is an arbitrary length of the tangents to the contours at a pressure ratio of 0.10.

TABLE I

Values of $\frac{r}{r_1}$, θ, ψ, m versus $\frac{p}{p_0}$.

p/p_0	θ°	$\frac{r}{r_1}$	ψ°	$m^\circ = (90-\psi)$
.527	0	1.000	0	90.000
.50	17.555	1.0483	17.120	72.880
.45	29.896	1.1474		
.40	39.306	1.2693	35.167	54.833
.35	48.152	1.4337		
.30	55.675	1.6242	45.735	44.265
.25	63.741	1.8989		
.225	67.892	2.0778		
.20	72.235	2.2992	54.176	35.824
.175	76.783	2.5780		
.15	81.677	2.9421	58.182	31.818
.125	87.554	3.4971		
.10	93.004	4.1648	62.383	27.617

VIII APPENDIX

C. Summary of Data.

TABLE II -(ρ/ρ_0)

1(a). Normal, shockless runs, upper contour.

Run	Atmos.	0.53	0.50	0.40	0.30	0.20	0.15	0.10	Date
1	764.4	0.578	0.519	0.420	0.367	0.232	0.198	0.143	7/26
2	765.5	0.573	0.515	0.416	0.381	0.214	0.189	0.143	"
3	764.6	0.578	0.517	0.470	0.369	0.248	0.164	0.151	7/29
4	"	0.578	0.517	0.442	0.369	0.248	0.164	0.140	"
5	"	0.575	0.516	0.448	0.375	0.239	0.190	0.140	"
6	"	0.576	0.516	0.436	0.372	0.240	0.189	0.141	"
7	764.5	0.576	0.518	0.492	0.380	0.236	0.192	0.149	8/2
8	759.0	0.574	0.516	0.506	0.385	0.237	0.200	0.159	8/10
9	764.4	0.568	0.509	0.425	0.364	0.236	0.186	0.150	8/12
10	"	0.569	0.514	0.429	0.364	0.232	0.186	0.147	"
Sum		5.745	5.157	4.485	3.726	2.362	1.858	1.463	
Avg.		0.574	0.516	0.448	0.373	0.236	0.186	0.146	

1(b). Normal, shockless runs, lower contour.

Run	Atmos.	0.53	0.50	0.40	0.30	0.20	0.15	0.10	Date
1	764.4	0.594	0.524	0.431	0.356	0.272	0.214	0.152	7/26
2	765.5	0.591	0.500	0.430	0.340	0.264	0.220	0.153	"
3	764.6	0.593	0.507	0.437	0.384	0.295	0.225	0.165	7/29
4	"	0.593	0.507	0.437	0.384	0.291	0.225	0.165	"
5	"	0.592	0.504	0.432	0.366	0.293	0.225	0.165	"
6	"	0.592	0.504	0.429	0.376	0.299	0.225	0.165	"
7	764.5	0.590	0.505	0.432	0.396	0.286	0.220	0.166	8/2
8	759.0	0.590	0.504	0.445	0.425	0.303	0.226	0.172	8/10
9	764.4	0.585	0.494	0.425	0.366	0.302	0.220	0.154	8/12

10	764.4	0.585	0.494	0.425	0.369	0.298	0.220	0.155	8/12
Sum		5.904	5.027	4.323	3.762	2.903	2.220	1.612	
Avg.		0.590	0.503	0.432	0.376	0.290	0.222	0.161	

2. Runs with shock in contour.

TABLE III $-(P/p_0)$

(a). Upper Contour.

Run	Atmos.	0.53	0.50	0.40	0.30	0.20	0.15	0.10	Date
I	759.0	0.574	0.516	0.506	0.385	0.237	0.200	0.159	8/10
II	764.4	0.569	0.505	0.420	0.359	0.229	0.295	0.357	8/12
III	764.5	0.566	0.505	0.419	0.359	0.291	0.439	0.430	8/12
IV	759.0	0.574	0.518	0.504	0.400	0.569	0.582	0.600	8/10
V	759.0	0.575	0.518	0.509	0.600	0.662	0.674	0.689	8/10
VI	759.0	0.580	0.545	0.646	0.720	0.769	0.781	0.792	8/10
VII	759.0	0.584	0.560	0.661	0.734	0.785	0.798	0.816	8/10

(b). Lower Contour.

Run	Atmos.	0.53	0.50	0.40	0.30	0.20	0.15	0.10	Date
I	759.0	0.590	0.504	0.445	0.425	0.303	0.226	0.172	8/10
II	764.4	0.584	0.490	0.422	0.361	0.301	0.215	0.224	8/12
III	764.5	0.583	0.491	0.424	0.360	0.301	0.215	0.351	8/12
IV	759.0	0.591	0.504	0.458	0.425	0.330	0.470	0.521	8/10
V	759.0	0.590	0.505	0.455	0.425	0.524	0.580	0.626	8/10
VI	759.0	0.595	0.515	0.491	0.695	0.656	0.706	0.744	8/10
VII	759.0	0.599	0.524	0.505	0.719	0.672	0.720	0.763	8/10

(Pictures corresponding to these runs marked Fig. 6-I, etc)

FIG. 6-I

FIG.6-II

FIG. 6-III

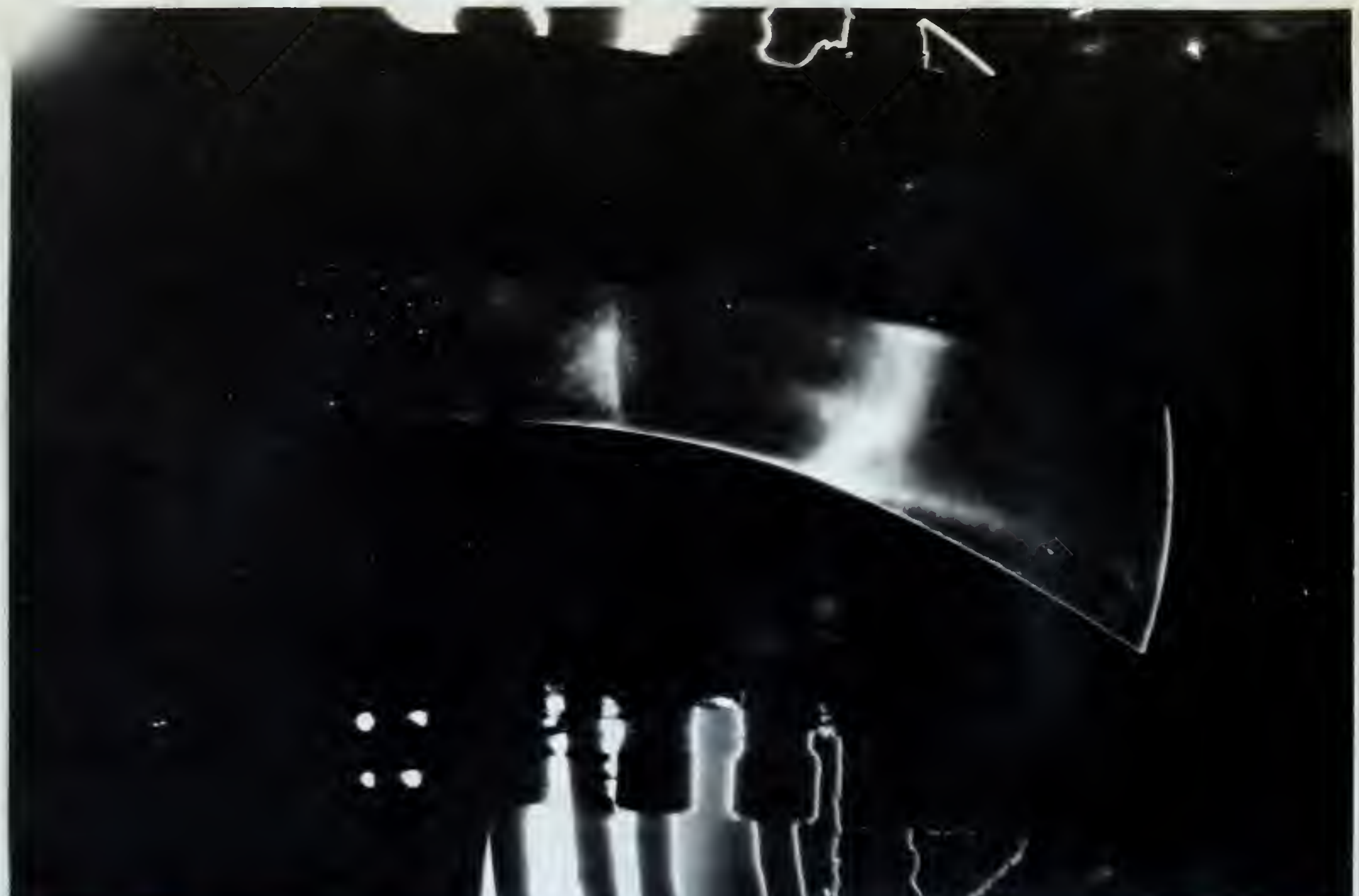

FIG. 6-IV

FIG. 6-V

FIG. 6-VI

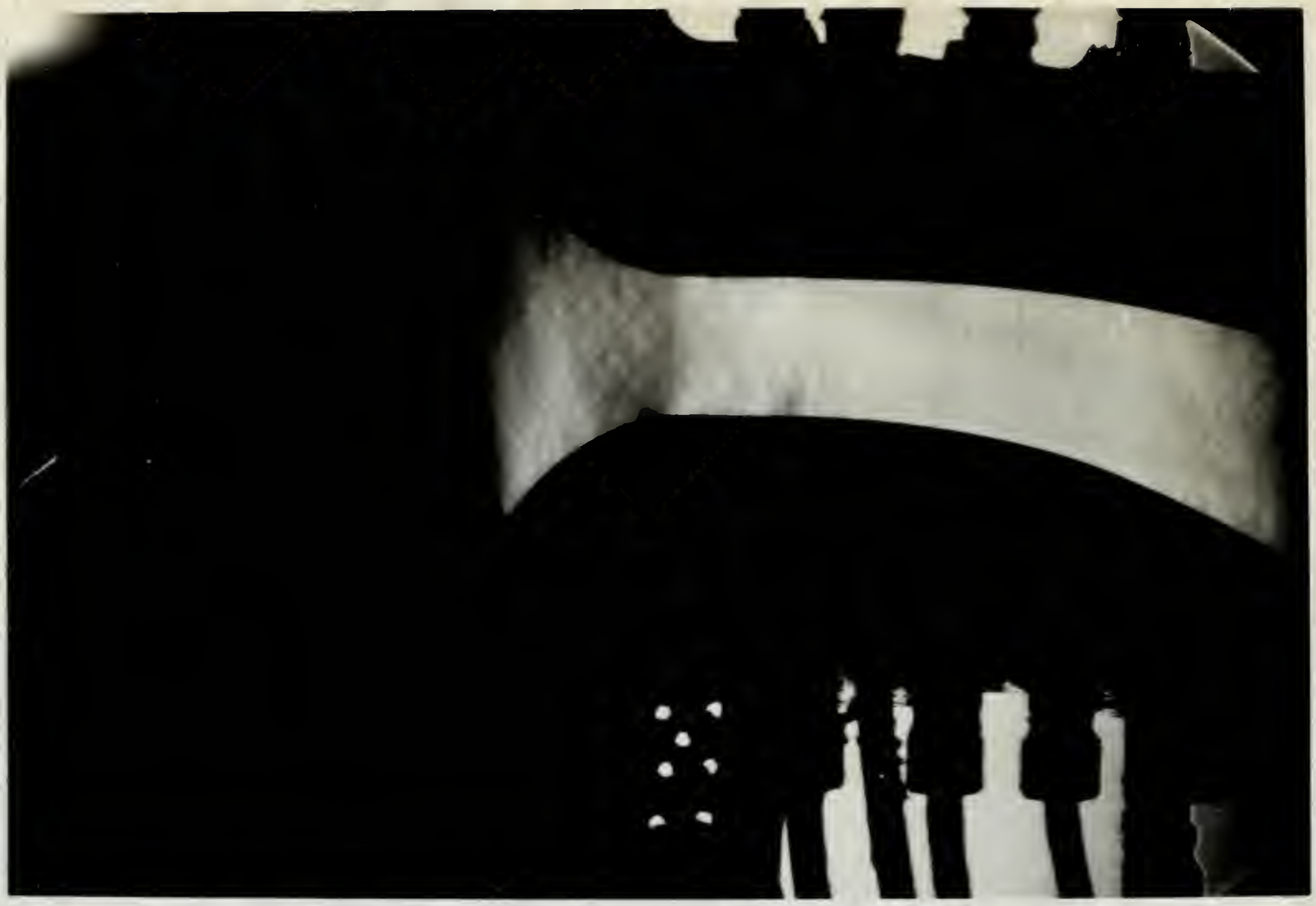

FIG. 6-VII

VIII APPENDIX

D. Sample Calculations.

1. Method of computing r/r_1, θ , ψ .

From appendix VIII, B:

$$r/r_1 = 0.57871\ (p/p_o)^{-0.85714}$$

$$\theta = 2.44949 \text{ arc cos } \left[1.0954(p/p_o)^{0.14286}\right]$$

$$\psi = \text{arc tan } \left(\frac{1}{\lambda} \tan \lambda\theta \right)$$

Assuming a pressure ratio of 0.40

	0.14286			log 9.15490-10
p_o/p =	2.500	log 0.39794	log	log 9.59981-10
		log 0.05685	log	log 8.75471-10
	1.0954			log 0.03959-
				-log 0.05685
	16.046°			logcos 9.98274-10
	16.046			log 1.20537
	2.4495			log 0.38908
θ =	39.306°			log 1.59445
	0.85714		log	log 9.93305-10
	2.500	log 0.39794	log	log 9.59981-10
		log 0.34108	log	log 9.53286-10
	0.57871	log 9.76246-10		
r/r_1 =	1.2693	log 0.10354		

D. Sample Calculations (con't).

For k = 1.400 $\sqrt{\frac{k-1}{k+1}} = 0.40825$

$\sqrt{\frac{k-1}{k+1}}$	= 0.40825	log	9.61092-10
θ	= 39.306	log	1.59445
		log	1.20537
	16.046°		
	16° 2.8'	logtan	9.45882-10
	2.4495	log	0.38908
ψ	= 35° 10.2'	logtan	9.84790-10

2. Calculation of pressure ratio.

Observed values, upper contour, mm Hg.

1.	Atmos.	0.53	0.50	0.40	0.30	0.20	0.15	0.10
2.	54	378	424	476	533	635	672	710
3.	Obs-Atm.	324	370	422	479	581	618	656
4.	Line 3 / Bar.	0.425	0.484	0.552	0.625	0.761	0.810	0.860
5.	p/p_o	0.575	0.516	0.448	0.375	0.239	0.190	0.140

3. Calculation of area perpendicular to flow.

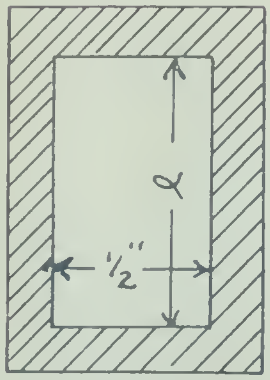

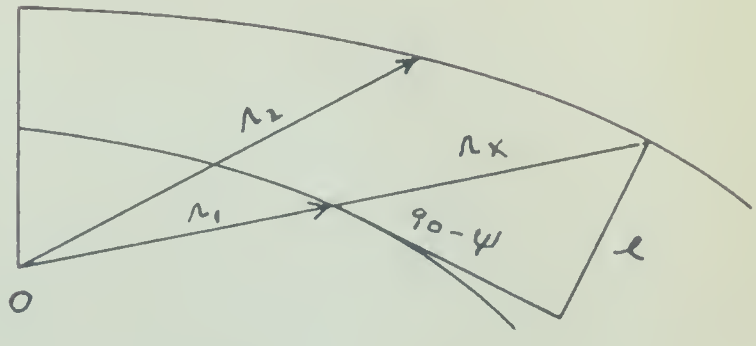

D. Sample Calculations (con't).

From sketch on preceding page:

$$r_x = r_1$$

$$A = \ell \cdot \frac{1}{2} = \frac{r_x \sin(90 - \psi)}{2}$$

Theo. p/p_o	0.53	0.50	0.40	0.30	0.20	0.15	0.10
r_x	1.000	1.0483	1.2693	1.6242	2.2992	2.9421	4.1648
$r_x/2$	0.500	0.5242	0.6346	0.8121	1.1496	1.4710	2.0824
$\sin(90-\psi)$	1.000	0.95569	0.81745	0.69804	0.58524	0.52725	0.46360
A in^2	0.500	0.50097	0.51875	0.56688	0.67279	0.77558	0.96540
A/A_t	1.000	1.002	1.039	1.132	1.346	1.552	1.930

4. Calculation of growth of boundary layer when layer is assumed to be uniform on all bounding surfaces.

(a). Upper contour.

Avg. p/p_o	0.574	0.516	0.448	0.373	0.236	0.186	0.146
M (for isen. exp. to avg. p/p_o)	0.93	1.02	1.14	1.28	1.60	1.76	1.92
A_t/A	0.996	0.998	0.990	0.950	0.800	0.720	0.635
A (req'd)	0.503	0.501	0.505	0.526	0.625	0.695	0.778
A (act.)	0.500	0.501	0.518	0.567	0.672	0.775	0.965
Diff. in^2		0.000	0.013	0.041	0.047	0.080	0.187
ℓ			1.036	1.132	1.344	1.550	1.930
t in.		0.000	0.0042	0.0126	0.0127	0.0195	0.0385

D. Sample Calculations (con't).

(b). Lower contour.

Avg. p/p_o	0.590	0.503	0.432	0.376	0.290	0.222	0.161
M	0.920	1.04	1.16	1.28	1.46	1.64	1.85
A_t/A	0.994	0.998	0.982	0.950	0.875	0.780	0.670
A (req'd)	0.504	0.501	0.509	0.526	0.571	0.641	0.746
A (act.)	0.500	0.501	0.519	0.567	0.673	0.775	0.965
Diff. in^2		0.000	0.010	0.041	0.102	0.134	0.219
ℓ			1.136	1.132	1.344	1.550	1.930
t in.			0;0033	0.0126	0.0277	0.0327	0.0450

$(\ell - 2t)(\tfrac{1}{2} - 2t) = A_{req'd}$

$4t^2 - t(2\ell+1) + \tfrac{1}{2}t = A_{req'd}$

Neglecting the t^2 term as insignificant.

$$t = \frac{\frac{1}{2}\ell - A(req'd)}{2\ell + 1} = \frac{A_{diff.}}{2\ell + 1}$$

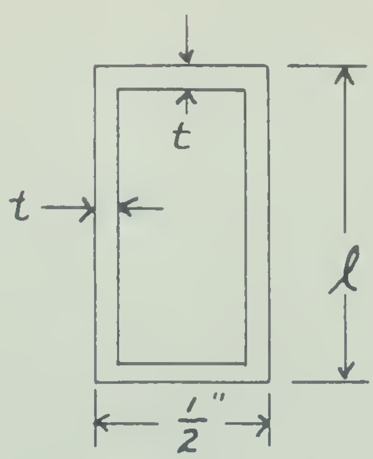

D. Sample Calculations (cont'd)

5. Calculation of new contour based on O'.

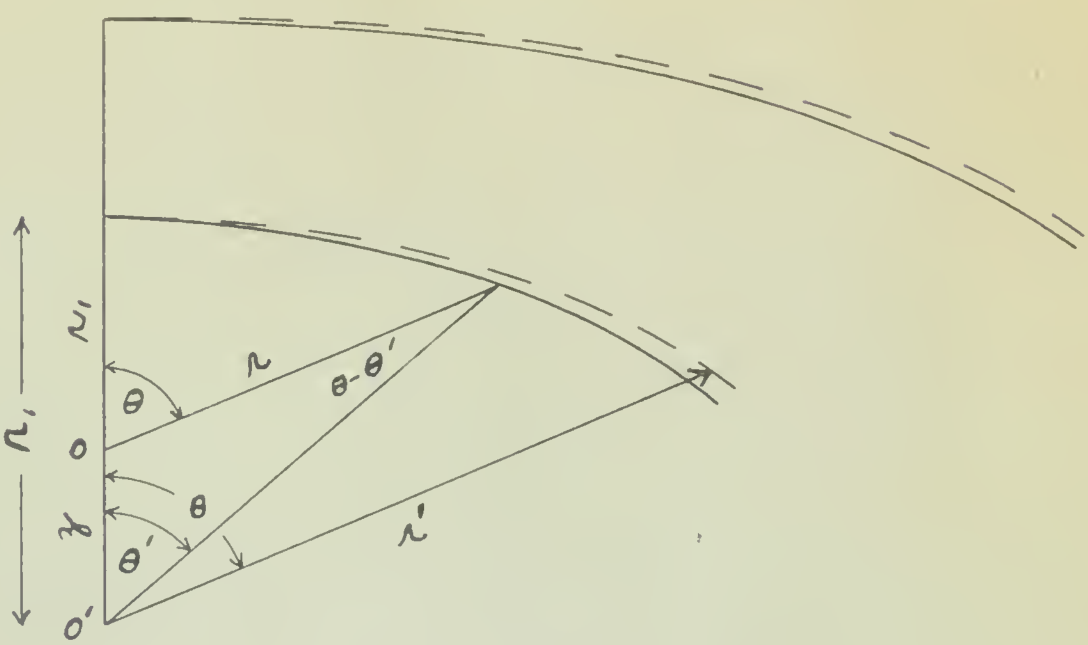

Equations used (from Appendix B and geometry of figure).

$$\theta' = 2.45 \cos^{-1}\left[1.095 \left(\frac{p}{p_o}\right)_{obs.}^{.1429}\right] \tag{1}$$

$$\gamma = r \frac{\sin(\theta - \theta')}{\sin \theta'} \tag{2}$$

$$r_1' = r_1 + \gamma \tag{3}$$

$$r' = r \frac{r_1'}{r_1} \tag{4}$$

Sample Calculation, Upper Contour, $\left(\frac{p}{p_o}\right)_{obs.} = .236$

$$\theta' = 2.45 \cos^{-1}\left[1.095\,(.236)^{.1429}\right] = 66.4^\circ$$

$$z = r\,\frac{\sin(\theta-\theta')}{\sin\theta'} = 4.60\,\frac{0.102}{0.916} = 0.513$$

$$r_1' = r_1 + z = 2.513$$

Calculated values based on observed pressure ratios.

THEO. p/p_0	0.53	0.50	0.40	0.30	0.20	0.15	0.10
				Upper Contour			
OBSERVED p/p_0	0.574	0.516	0.443	0.373	0.236	0.186	0.146
θ'	0	11.75	31.1	44.4	66.4	74.6	82.8
z	0	0.104	0.698	0.910	0.513	0.756	1.49
r_1'	2.00	2.104	2.698	2.910	2.513	2.756	3.49
r'	2.00	2.20	3.42	4.71	5.77	8.09	14.50
θ	0	17.55	39.31	55.67	72.24	81.67	93.00
				Lower Contour			
OBSERVED p/p_0	0.590	0.503	0.432	0.376	0.290	0.222	0.161
θ'	0	15.2	33.6	44.4	57.1	68.1	79.6
z	0	0.164	0.227	0.456	0.715	0.748	0.981
r_1'	1.00	1.164	1.227	1.456	1.715	1.748	1.981
r'	1.00	1.22	1.55	2.37	3.95	5.14	8.26
θ	0	17.55	39.31	55.67	72.24	81.67	93.00

A plot of the values of r' and θ gives the contour shown by the dotted lines in the figure on the preceding page.

VIII APPENDIX

F. Supplementary Discussion.

1. Interpretation of pictures.

The condensation shock, Fig. 6-I, was present for normal flow and for shocks downstream of it. Its slope did not agree with the slope of the theoretical lines of constant pressure nor with the slope of the pressure shocks.

Fig. 6-II and Fig. 6-III show a peculiar type of shock occuring well downstream. Separation is quite apparent here.

Fig. 6-IV and Fig. 6-V show the shock approaching the condensation shock.

Fig. 6-VI shows a pressure shock occuring in the vicinity of the condensation shock. Separation at the lower contour is noticeable. Most of the light area downstream is caused by imperfections in the glass.

Fig. 6-VII was taken with the shock upstream of the throat section. Note that the condensation shock seems to have disappeared in this condition of flow.

Pressure shocks were not stationary but moved back and forth quite rapidly, creating a wide band in the photographs. The camera used in taking these photographs was not fast enough to stop the motion of the shocks.

VIII APPENDIX

F. Location of Original Data.

All original calculations, graphs, and negatives are in the possession of Professor Ernest P. Neumann of the Mechanical Engineering Department, Massachusetts Institute of Technology.

VIII APPENDIX

G. Literature Citations.

(1) W. F. Durand---"Aerodynamic Theory" Vol. III p.243.

(2) F. H. Clauser--"Aerodynamics of Ducted Bodies at Supersonic Speeds." Bumblebee Report No. 29, CONFIDENTIAL, pps. 29-38.

(3) L. A. DeFrate--"Investigation of Supersonic Flow in Nozzles and Tubes." M.S. Thesis in M. E. 1943, MIT.

(4) R. Hermann---"Condensation Shock Waves in Supersonic Wind Tunnel Nozzles." LUFTFAHRTFORSCHUNG, Vol. 19, No. 6 pps. 201-209.

(5) J. H. Keenan--"Thermodynamics", John Wiley & Sons, Inc. 1941.

(6) J. H. Keenan and J. Kaye--"Thermodynamic Properties of Air". John Wiley & Sons, Inc. 1945

11664
Thesis H445
Hennessey
An experimental study of flow in a nozzle designed to produce (provide) a parallel jet at supersonic speed.